Proton Tunneling in Aromatic Amine Dehydrogenase is Driven by a Short-Range Sub-Picosecond Promoting Vibration: Consistency of Simulation and Theory with Experiment

Linus O. Johannissen,[†,‡] Sam Hay,[†,§] Nigel S. Scrutton,[†,§] and Michael J. Sutcliffe*[,†,‡]

Manchester Interdisciplinary Biocentre, School of Chemical Engineering and Analytical Science, and Faculty of Life Sciences, University of Manchester, 131 Princess Street, Manchester M1 7DN, U.K.

Received: September 25, 2006; In Final Form: November 30, 2006

Hydrogen transfer, an essential component of most biological reactions, is a quantum problem. However, the proposed role of compressive motion in promoting enzymatic H-transfer is contentious. Using molecular dynamics simulations and density functional theory (DFT) calculations, we show that, during proton tunneling in the oxidative deamination of tryptamine catalyzed by the enzyme aromatic amine dehydrogenase (AADH), a sub-picosecond promoting vibration is inherent to the iminoquinone intermediate. We show by numerical modeling that this short-range vibration, with a frequency of ∼165 cm^{-1}, is consistent with "gating" motion in the hydrogen tunneling model of Kuznetsov and Ulstrup (Kuznetsov, A. M.; Ulstrup, J. *Can. J. Chem.* **1999**, *77*, 1085) in an enzymatic reaction with an observed protium/deuterium kinetic isotope effect that is not measurably temperature-dependent.

Introduction

The importance of hydrogen tunneling in enzyme catalyzed reactions, and in particular the role of protein motion in facilitating the H-tunneling process—by short-range conformational changes within the active site and possible coupling of these local changes to longer range conformational changes—has been intensely debated.[1−13] A key experimental indicator of enzymatic H-tunneling is the magnitude and temperature-dependent behavior of kinetic isotope effects (KIEs).[14] Such kinetic data,[13,15−25] which can be explained by neither conventional transition state theory nor the Bell tunneling correction to transition state theory,[26] are in agreement with environmentally coupled models of H-tunneling[20,27,28] and can be simulated computationally[29−37] within the framework of modern transition state theory[38] using different approaches involving either quantum mechanical/molecular mechanical (QM/MM)[28] or empirical valence bond (EVB)[4,39] potentials. In the Kuznetsov and Ulstrup environmentally coupled model of H-tunneling,[27] as used quantitatively by Klinman and co-workers,[20] temperature-independent KIEs arise from Marcus-like vibrations (collective thermally equilibrated motions) that lead to degenerate reactant and product states, while temperature-dependent KIEs arise from "gating motions" (motion along the reaction coordinate, i.e., motion along and coupled to the hydrogen coordinate) that enhance the probability of tunneling at this configuration by bringing the reactant and product wells closer together.

The quinoprotein enzymes, the mechanisms of which are generally well understood, are ideally suited to studies of H-transfer during substrate oxidation,[40] and are thus excellent systems for investigating H-transfer by nuclear tunneling. H-tunneling in the quinoprotein methylamine dehydrogenase (MADH), which involves transfer of a proton from a C−H bond of a substrate-derived iminoquinone intermediate to the catalytic base, has been studied both experimentally[15,16] and computationally.[30−34,41] We have also studied the kinetics of proton tunneling with a range of substrates, and the importance of barrier shape in determining reaction rate, in the related quinoprotein aromatic amine dehydrogenase (AADH).[16] We recently published a combined kinetic, crystallographic, and computational study of H-tunneling in AADH, which involves the transfer of a proton from a C−H bond of a tryptamine-derived iminoquinone intermediate to the catalytic base, Asp128β. The kinetic data[13] reveal a protium/deuterium KIE that is not measurably temperature-dependent (55 ± 6; the temperature dependence is smaller than the error bars over the 5−20 °C temperature range for which there are data on both H and D isotopologues) and inflated well beyond the semiclassical limit and near-identical phenomenological enthalpies of activation for protiated and deuterated substrate ($\Delta H^{\ddagger H} = 57.3 \pm 3.4$ kJ mol^{-1}, $\Delta H^{\ddagger D} = 53.5 \pm 1.2$ kJ mol^{-1}). Computational simulations could only successfully reproduce the experimental rate by incorporating tunneling, which increases the rate by 3 orders of magnitude (i.e., in excess of 99.9% of proton transfers occurs via tunneling).[13] On the basis of the proton−acceptor distances in the reactant structure (**III** in Figure 2a), tunneling could conceivably occur to either carboxyl oxygen of Asp128β. However, crystallography suggests that transfer to one of these oxygens (i.e., O2) is mechanistically more likely,[13] and the computational simulations, which employed variational transition state theory with small-curvature multidimensional tunneling corrections, indicate that tunneling to O2 is favored both kinetically and thermodynamically.[13]

Our study[13] revealed that progressing from (i) the reactant to (ii) the representative structure for tunneling to O2 (RTE structure) requires significant heavy atom motion (and no C−H bond stretching), involving rotation of donor carbon (C1) and

* To whom correspondence should be addressed. Phone: +44 161 306 5153. Fax: +44 161 306 8918. E-mail: michael.sutcliffe@manchester.ac.uk.
† Manchester Interdisciplinary Biocentre.
‡ School of Chemical Engineering and Analytical Science.
§ Faculty of Life Sciences.

10.1021/jp066276w CCC: $37.00
Published on Web 02/17/2007

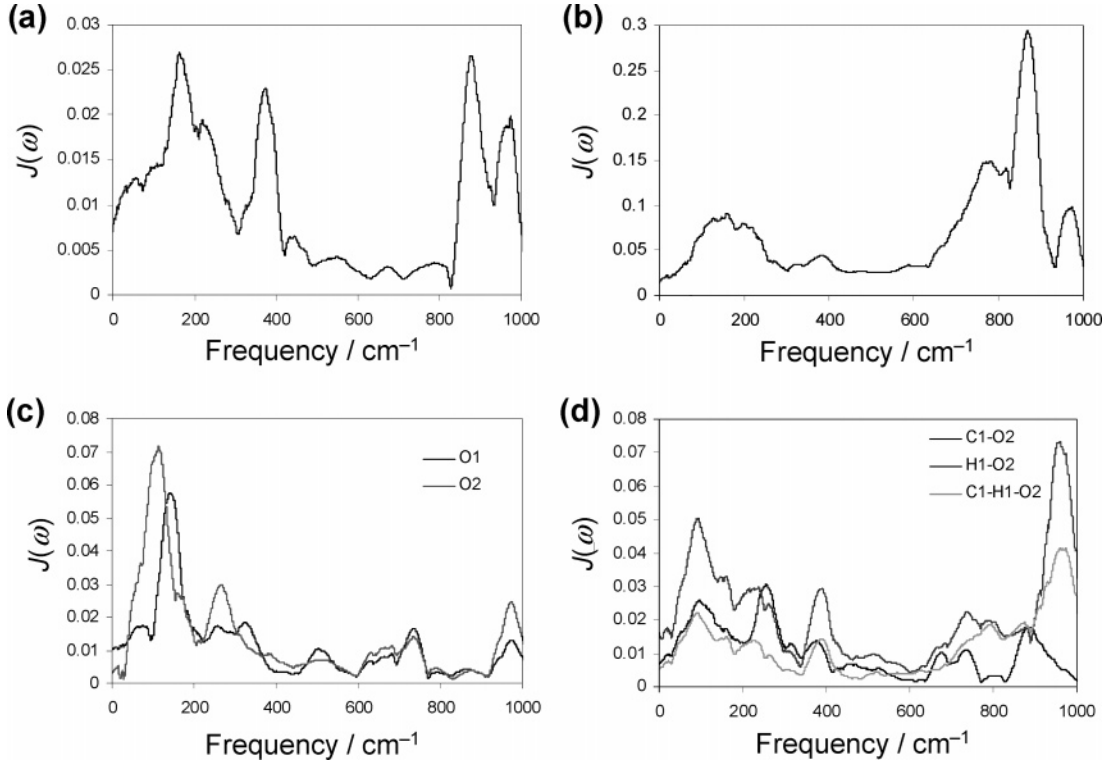

Figure 1. Velocity spectral densities for (a) C1, (b) H1, and (c) O1/O2; (d) relative-velocity spectral densities for C1/H1−O2 and reaction-coordinate spectral density for C1−H1−O2.

the transferring hydrogen (H1) accompanied by a repositioning of O2. These "R-to-RTE" (where R is the reactant) motions correspond to the structural changes occurring along the minimum energy path for the proton transfer reaction and are therefore a good representation of the reaction coordinate leading up to the tunneling event (i.e., the motions along and coupled to the hydrogen coordinate; this definition for the reaction coordinate is employed throughout the paper, unless otherwise stated). Our study showed that, in this enzyme system, tunneling is promoted by a short-range vibration, with a frequency of ~165 cm^{-1}, modulating the proton−acceptor distance. In this study, we further characterize this motion through analysis of the molecular dynamics trajectory and numerical modeling based on the framework of the Kuznetsov and Ulstrup model.[27]

Methods

Dynamics Simulations. 7 ns MM (CHARMM22) molecular dynamics were performed for the $\alpha_2\beta_2$ heterotetramer for the modeled iminoquinone structure,[13] including crystal waters. Dynamical cross-correlation analysis[42] was performed on the last 5 ns of the trajectory, after ensuring that the correlation coefficients had converged. Spectral densities[43] of the motions were calculated for a 400 ps window (2.0−2.4 ns) with coordinates recorded every 4 fs. Digital filtering by frequency deconvolution[44] was applied to the same 400 ps window to obtain atomic velocities for a selected frequency range (i.e., 165 ± 30 and 100 ± 30 cm^{-1}). To gain insight into how the atoms move during the MD simulation, these new velocities were applied to the coordinates in the first frame of the MD trajectory. To compare these movements with those observed in our VTST calculations,[13] the coordinates in this first frame were structurally aligned with the minimized R structure from the VTST calculations using atoms in the linker region connecting the quinone and the indole and the side chain of Asp128β (Supporting Information Figure S1). QM frequency calculations were carried out using Gaussian 98, with initial energy minimization carried out at the B3LYP/6-31G* level, both with and without the relative orientations of the quinone and indole rings[13] fixed.

Measuring the Strength of Coupling of Specific Vibrational Frequencies. The strength of the coupling, C, was defined as

$$C(f_1 - f_2) = C_\tau(f_1 - f_2) \times \left[1 - \frac{|V(f_1 - f_2) - C_\tau(f_1 - f_2)|}{\max[V(f_1 - f_2), C_\tau(f_1 - f_2)]}\right] \quad (1)$$

where $V(f_1 - f_2)$ is defined as the velocity spectral density and $C_\tau(f_1 - f_2)$ as the time-correlation spectral density[45] for the frequency range $f_1 - f_2$. $V(f_1 - f_2)$ and $C_\tau(f_1 - f_2)$ are both relative to the area in the same frequency range for the C1 velocity spectral density, since they serve to measure the extent to which a given atom pushes C1. The term in the square brackets in eq 1 serves to normalize $C_\tau(f_1 - f_2)$ so that $0 \leq C(f_1 - f_2) \leq 1$ (see the Supporting Information for more details). The time-correlation function for atom A and C1 is given by

$$C_{A,C1}(i) = \langle v_A(t + i) \cdot v_{C1}(t) \rangle \quad (2)$$

Both $C_{A,C1}(i)$ and $C_{C1,A}(i)$ were calculated and averaged to give $C(i)$, whose autocorrelation function was then Fourier transformed to give the time-correlation spectral density.

Numerical Modeling. The experimentally determined kinetic properties of AADH/tryptamine have been described previously.[13] In brief, these are KIE = 55 ± 6, $\Delta H^{\ddagger}_{obsd}{}^{H} = 57.3 \pm 3.4$ kJ mol^{-1}, $\Delta H^{\ddagger}_{obsd}{}^{D} = 53.5 \pm 1.2$ kJ mol^{-1}, $\ln(A')^{H} = 25.6 \pm 1.4$, and $\ln(A')^{D} = 19.79 \pm 0.49$. In this study, we use a value for $\Delta\Delta H^{\ddagger}$ ($\Delta H^{\ddagger D} - \Delta H^{\ddagger H}$) of ~0 ± 5 kJ mol^{-1}. Additionally, we do not attempt to "fit" the A'^{H}/A'^{D} ratio, as the experimentally determined value, $A'^{H}/A'^{D} = 334 \pm 631$, is not useful due to the large error.

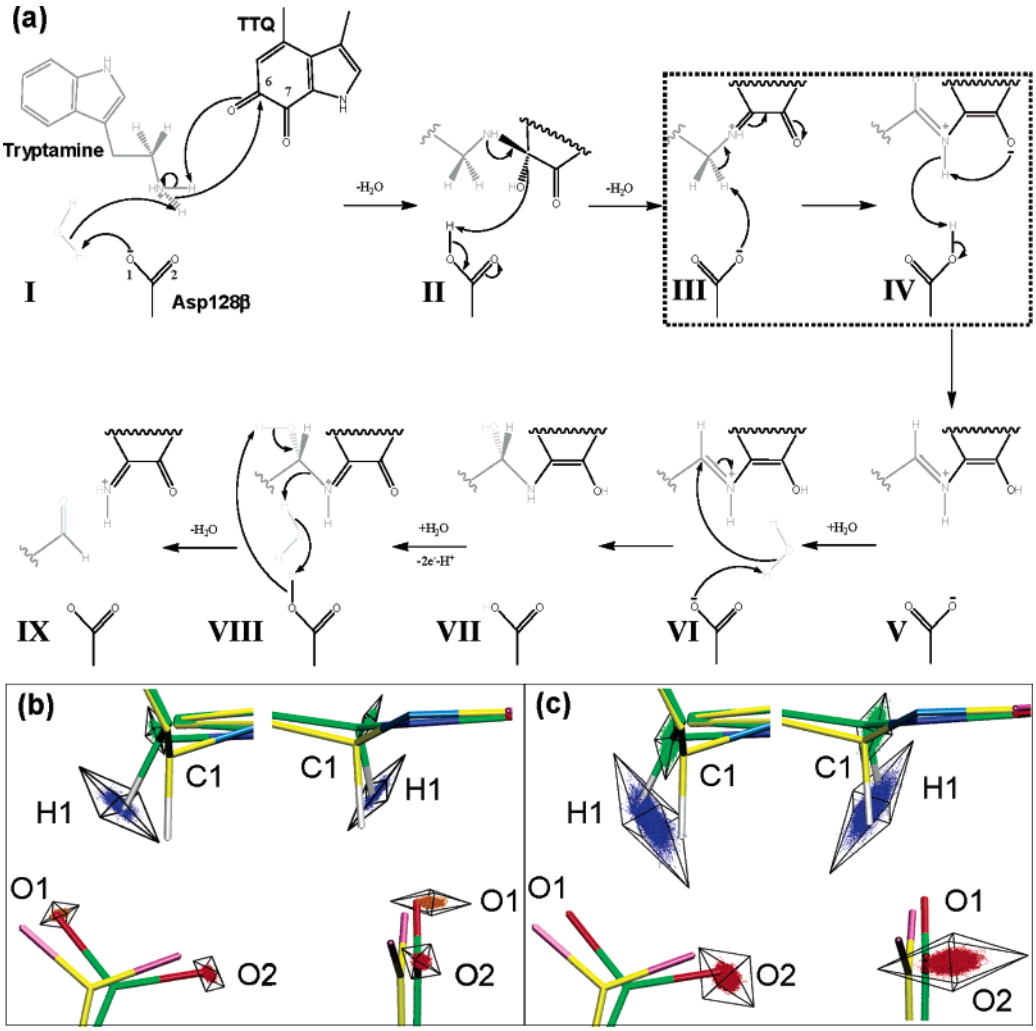

Figure 2. (a) Schematic overview of the reaction mechanism of the reductive half-reaction of AADH with tryptamine.[13] Atoms derived from the substrate are depicted in dark gray, and those derived from water, in light gray. All other enzyme-derived atoms are depicted in black; the catalytic base, Asp128β, is labeled in **I**. The proton transfer (H^+-tunneling) step is boxed; **III** and **IV** refer to the reactant and product of the proton transfer step, respectively. (b and c) Orthogonal views of the reactant (green carbon atoms) and the RTE (yellow carbon atoms) structures from previous VTST calculations,[13] with superimposed atomic coordinates for the (b) ~165 cm^{-1} and (c) ~100 cm^{-1} vibrations for C1, H1, O1, and O2. The cages represent the principal components for the filtered motion of each atom and are scaled according to the relative eigenvalues.

Within the framework of the Kuznetsov and Ulstrup model, the complete rate equation for ground state tunneling[20] is given by

$$k_{\text{tunnel}(0,0)} = \left[\frac{1}{2\pi}\left|V_{\text{el}}\right|^2\sqrt{4\pi^3/\lambda RT\hbar^2}\right]\exp\left\{\frac{-(\Delta G^\circ + \lambda)^2}{4\lambda RT}\right\} \times \text{(FC term)} \quad (3)$$

where V_{el} is the isotope-independent electronic coupling constant and was optimized to give the best fit to the experimental rates. The reorganization energy, λ, was also estimated by fitting the data to the rate equation; altering λ directly affects the $\Delta H^{\ddagger}$ values. For tunneling through a static barrier (assuming no contribution from excited C1−H1 vibrational states), the Franck−Condon (FC) term is given by

$$\text{FC}_i = \exp(-\mu_i\omega_i r^2/2\hbar) \quad (4)$$

where μ_i is the reduced mass, ω_i is the angular frequency of the transferred isotope, and r is the tunneling distance, that is, the distance between the reactant and product wells at a nuclear configuration compatible with tunneling. The FC term assumes that the proton is transferred from the vibrational ground state of the C1−H1 bond; this assumption is not necessarily valid and will be addressed further on. To simplify the calculations, μ_i was calculated as the average C/O−H/D reduced mass (μ_{H} = 0.94 g mol^{-1}, μ_{D} = 1.75 g mol^{-1}) and ω_i as the average angular frequencies ($\omega_{\text{H}} = 5.65 \times 10^{14}$ s^{-1}, $\omega_{\text{D}} = 4.14 \times 10^{14}$ s^{-1}) calculated from the stretching frequencies $f_{\text{H}} = 3000$ cm^{-1} and $f_{\text{D}} = 2200$ cm^{-1}. The KIE increases with Δr (Figure 6, Table 1), and a KIE of 55 occurs when $\Delta r = 0.51$ Å. This value is significantly shorter than the tunneling distance of 0.59 Å obtained from the VTST/MT calculations.[13] The KIE is very sensitive to the tunneling distance, so even allowing for a KIE of 60, the Δr value only increases to 0.52 Å. Therefore, while this model allows a good fit to the experimental data, it requires a tunneling distance that is significantly shorter than the computationally derived value. Since there is no temperature dependence on the KIE, the ratio of Arrhenius prefactors in this case is $A_{\text{H}}/A_{\text{D}}$ = KIE = 55.

To account for the possibility of tunneling from and/or to a vibrationally excited state (i.e., from the C1−H1 excited state and/or to an O2−H1 excited state), expressions for vibrational state specific Franck−Condon overlaps[20] were employed. In

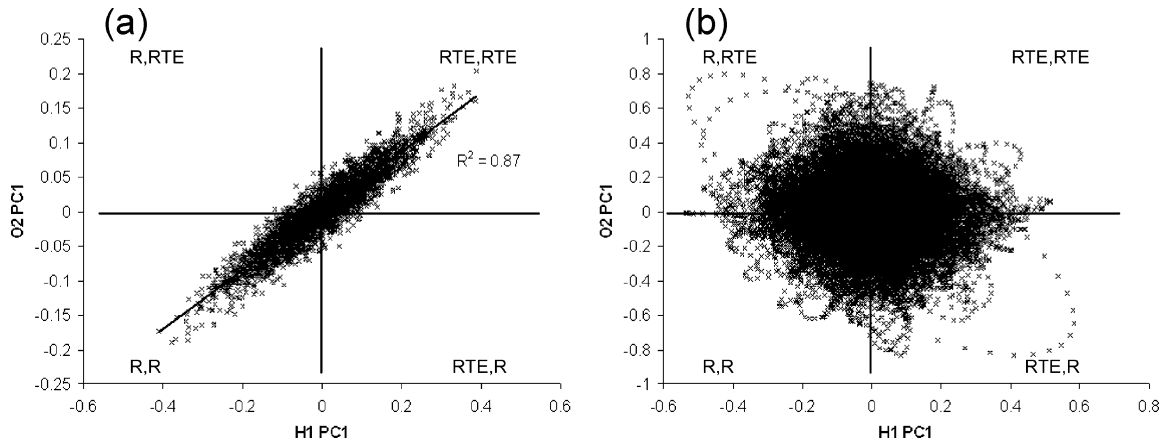

Figure 3. Correlation between PC1 for H1 and PC1 for O2 for (a) the ~165 cm^{-1} vibration and (b) the ~100 cm^{-1} vibration. "R" corresponds to the reactant structure and "RTE" to the representative structure for tunneling to O2.

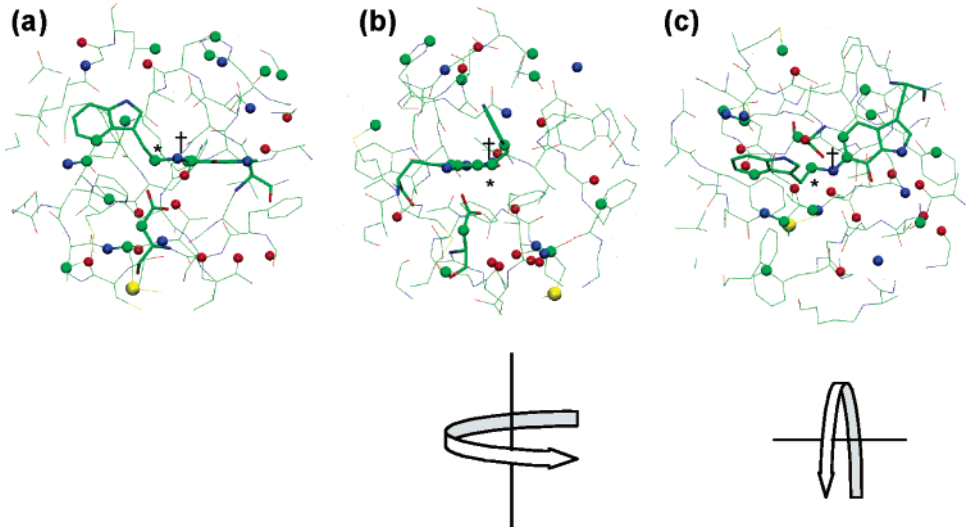

Figure 4. Orthogonal views of atoms surrounding C1 with $C(135-195) > 0.5$. All of the atoms used in the analysis are shown as lines, the iminoquinone and Asp128β as thicker lines, and the atoms with $C(135-195) > 0.5$ as spheres. The diagrams below views b and c illustrate how each is obtained from rotation of a. C1 is designated by * and N1 by † (N1 is directly behind C1 in part b).

each case, tunneling is assumed to occur between oscillators of equal frequencies:

$$FC_{0,0} = \exp(-\mu\omega r^2/2\hbar) \quad (5)$$

$$FC_{0,1} = (\mu\omega r^2/2\hbar) \times \exp(-\mu\omega r^2/2\hbar) \quad (6)$$

$$FC_{1,0} = (\mu\omega r^2/2\hbar) \times \exp(-\mu\omega r^2/2\hbar) \quad (7)$$

$$FC_{1,1} = (1 - \mu\omega r^2/2\hbar)^2 \times \exp(-\mu\omega r^2/2\hbar) \quad (8)$$

where $FC_{i,j}$ is the FC term for tunneling from vibrational state i to vibrational state j. Note that for simplification only the first vibrationally excited states are included (the Boltzmann populations of the higher excited states are negligible). Each FC term for each transition must be weighted according to the Boltzmann populations, P_i:

$$k_{\text{tunnel}} = \sum_i P_i \sum_i \frac{1}{2\pi} |V_{\text{el}}|^2 \sqrt{4\pi^3/\lambda RT\hbar^2} \times \exp\left\{\frac{-(\Delta G^\circ + E_{\text{vib}} + \lambda)^2}{4\lambda RT}\right\} \times (FC_{i,j}) \quad (9)$$

where E_{vib} is the difference in vibrational energy between the reactants and products: ~36 and 26 kJ mol^{-1} for H and D, respectively, at room temperature. Again, the experimental data can be accommodated by this model (Table 1), but the r value is at variance with the computationally derived value.

In the case where the tunneling probability is modulated by a promoting vibration (gating), the FC term becomes

$$FC_i = \int_0^{r_0} \exp(-\mu_i\omega_i\Delta r^2/2\hbar) \exp(-E_X/k_BT)\, dX \quad (10)$$

$$E_X = \frac{1}{2}\hbar\omega_X X^2 \quad (11)$$

$$X = r_X\sqrt{m_X\omega_X/\hbar} \quad (12)$$

All other terms in the rate equation (eq 3) are isotope-independent, so the KIEs arise from the ratios of the Franck−Condon terms for proton and deuteron transfer.[14] The gating mode is treated as an isotope-independent harmonic oscillator with energy E_X. The frequency term ω_X is now the angular frequency of the gating motion along the reduced gating coordinate, X. The gating "unit" has a mass, m_X, with a force constant, $k_{HO} = m_X\omega_X^2$. The tunneling distance at a nuclear configuration compatible with tunneling is r_0, and the gating

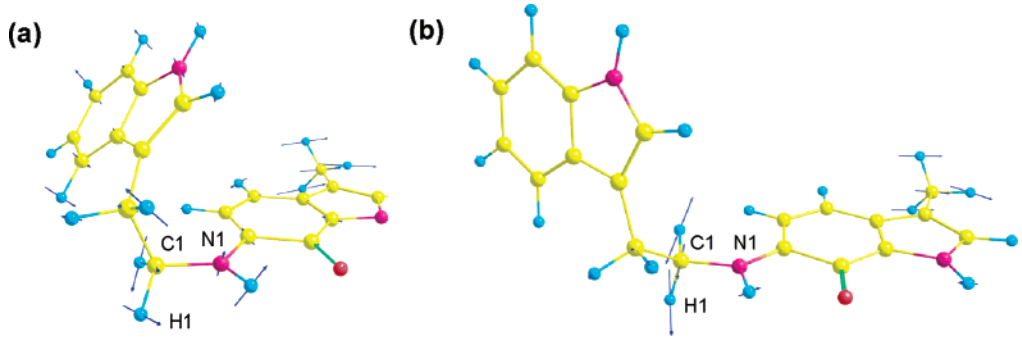

Figure 5. B3LYP/6-31G* energy minimized iminoquinone structure, with scaled arrows representing the vibration for the C1/H1 rotation: (a) without any constraints (174 cm^{-1}); (b) with indole/quinone orientations fixed (164 cm^{-1}).

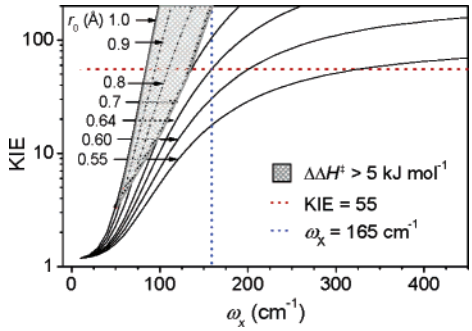

Figure 6. Implementation of the Kuznetsov and Ulstrup model (eqs 9 and 10) showing the effect of the gating frequency, ω_X, on the KIE at 298 K for a range of r_0 values, when $m_X = 100$ Da.

term reduces this tunneling distance by r_X; the gated tunneling distance is $\Delta r = r_0 - r_X$. The root-mean-square (rms) displacement of r_X is

$$r_{\text{displacement}} = \sqrt{k_B T / k_{HO}} \tag{13}$$

Results and Discussion

To determine whether specific enzymatic vibrations push the system along the reaction coordinate, spectral density analysis[43,46] of a molecular dynamics simulation of the reactant structure was carried out. The spectral densities obtained for the C1 and H1 velocities (Figure 1a,b) show a common peak at ~165 cm^{-1}, and O2 has a "shoulder" peak at ~165 cm^{-1} (Figure 1c). This suggests the possibility that the ~165 cm^{-1} vibration common to C1, H1, and, to some extent, O2 corresponds to the reorganization that occurs as the system moves from R to the RTE configuration. The three-dimensional nature of this vibration was determined by digital filtering by frequency deconvolution[44] to remove motions outside a ±30 cm^{-1} window around this frequency, followed by mapping the resulting coordinates onto the reactant structure. This revealed that this vibration does indeed correspond to the structural changes that occur with C1, H1, and O2 in passing from the R to the RTE structure (Figure 2b, Supporting Information Table S1), which suggests that this vibration might correspond to a promoting vibration. However, a promoting vibration must be symmetrically coupled to the reaction coordinate;[47−49] the vibration will only push the system toward the tunneling configuration and concomitantly reduce the barrier height[48] if the acceptor moves toward the RTE structure synchronously with the donor and transferring proton. Principal component analysis of the filtered motion for O2 and H1 revealed that these two atoms move synchronously toward and away from the RTE structure at ~165 cm^{-1} (Figure 3). The ~165 cm^{-1} vibration of C1/H1 is therefore coupled to the vibration of O2 at the same frequency, presumably by electrostatic interaction or weak hydrogen bonding, and promotes tunneling to O2. As C1/H1 and O2 are pushed together toward a "tunneling-ready" configuration, the secondary hydrogen on C1 becomes more in plane with the iminoquinone nitrogen and the C1−H1 bond orbital becomes more perpendicular to the plane of the iminoquinone, thus making sp^3 hybridized C1 more product (sp^2)-like and further increasing the probability of tunneling of H1.

The relative-velocity and reaction-coordinate spectral densities, as employed by Schwartz and co-workers to diagnose a 150 cm^{-1} promoting vibration in hLADH,[43] were obtained for C1, H1, and O2 (Figure 1d). In this case, a simplified reaction coordinate is used, defined as the position of the hydrogen relative to the donor−acceptor center of mass projected onto the donor−acceptor axis.[43] Nevertheless, motion along the R-to-RTE vectors will present itself as motion along this simplified reaction coordinate. The strongest low-frequency peaks correspond to an ~100 cm^{-1} vibration (together with a shoulder at ~165 cm^{-1}). The vibration of H1 at this frequency lies closer to the H1−O2 interatomic axis (Figure 2c) than the corresponding ~165 cm^{-1} vibration. However, since C1, H1, and O2 are not collinear in the reactant, the promoting vibration is not necessarily that for which the individual atomic vibrations lie closest to the interatomic axes. While the 100 cm^{-1} vibration modulates the C1/H1−O2 separation, the motions of H1 and O2 are not coupled to the reaction coordinate (Figure 3b, Supporting Information Table S1) and it is therefore not a promoting vibration.[43,46] Nevertheless, such thermally equilibrated motions have previously been shown to be important for reducing the donor−acceptor distance below its equilibrium value which is required for efficient tunneling, as well as altering the electrostatic environment.[35,50−52] In this case, the 100 cm^{-1} vibration appears to be necessary to bring O2 sufficiently close to H1 for the 165 cm^{-1} vibration of H1 to couple to that of O2, bringing O2 and H1 even closer (Figure 2b versus Figure 2c). This illustrates the importance of taking into account the three-dimensional nature of the reaction coordinate.

Previously, we noted that the overall motion of C1/H1 is not coupled to any other motion,[13] based in part on the principal component analysis of the covariance matrix of the reacting groups from a 4 ns portion of a molecular dynamics simulation. Although this is apparently at odds with the above discussion, it should be noted that the ~165 cm^{-1} vibration contributes relatively little to the overall motion of O2; thus, while this vibration is coupled to the C1/H1 vibration, the overall motion of O2 is not. Furthermore, the cross-correlation analysis for the β subunit (Supporting Information Figure S2), which encompasses the iminoquinone and Asp128β, shows no regions of strong correlation, suggesting that long-range coupled motions

TABLE 1: Parameters for Modeling the Experimental Rates of Tryptamine Oxidation by AADH within the Framework of the Kuznetsov and Ulstrup Model

	$-\Delta G°$ (kJ/mol)	λ (kJ/mol)	r/r_0[a] (Å)	ω_X (cm^{-1})	m_X (Da)	$\Delta H^{\ddagger H}$ (kJ/mol)	$\Delta H^{\ddagger D}$ (kJ/mol)	KIE (25 °C)
static barrier[b]	32.6	297	0.51			55.0	55.0	55
	32.6	297	0.52			55.0	55.0	60
static barrier[c]	32.6	288	0.52			53.1	54.2	55
	32.6	288	0.53			53.1	54.2	60
gating	32.6	252	0.64	165	100	51.2	54.9	55
	32.6	252	0.65	165	100	51.2	55.0	60
experimentally determined values[13]						57.3 ± 3.4	53.5 ± 1.2	55 ± 6
computationally determined values[13]	32.6		0.59					

[a] r values are given for the static barrier models, and r_0 for the gating model. [b] No contribution from excited states (eqs 3 and 4). [c] Contribution from the first reactant and product excited states.

are not likely to be significant (although we do not rule out stochastic motions).

As well as analyzing the correlation of the *overall* motions of the atoms and residues of interest, we also investigated whether there is a coupling between the promoting vibration and the ~165 cm^{-1} vibrations of atoms surrounding C1. The velocity and time-correlation spectral densities[45] for all heavy atoms that remain within 12 Å of C1 during the MD simulation were calculated, and the strength of the coupling was measured as the area under the latter normalized according to the area under the former for the ±30 cm^{-1} range employed previously.[13] The resulting coupling coefficients, C, range from 0 to +1, with a coupling of +1 indicating that the vibration is parallel to that of C1, with a magnitude greater than or equal to that of C1. This analysis revealed no network of coupled motions, and apart from three atoms within the quinone, those atoms with $C >$ 0.5 are too distant to transfer their vibrational energy to C1 (Figure 4). That the promoting vibration is inherent to the iminoquinone moiety and does not arise from vibrations of the enzyme is further supported by quantum mechanical gas phase frequency calculations at the B3LYP/6-31G* level (Figure 5). The structure of the iminoquinone is constrained in the enzyme active site, so the initial energy minimization caused a significant change in the geometry. Nevertheless, a similar vibration, corresponding to a C1/H1 rotation, was observed at a similar frequency of 174 cm^{-1}. To mimic the constraining effect of the enzyme, the iminoquinone was then energy minimized with the relative orientations of the indole and quinone rings of the iminoquinone fixed; the resulting structure is a nonstationary point on the potential energy surface, but it has previously been shown that fixing certain atoms is a suitable method to mimic the strain of the enzyme.[53] This gave a frequency of 164 cm^{-1} for the C1/H1 rotation.

The computationally derived promoting vibration and the experimentally observed tunneling kinetics fit adequately within the formulism of the Kuznetsov and Ulstrup model[20,27] (Table 1), in which gating is described as a simple harmonic oscillator. In this model, the KIE arises from the Frank−Condon terms of the transferring isotopes. A prerequisite for this model is that the system involves deep tunneling, that is, that the reaction proceeds entirely via tunneling. AADH therefore seems to be an ideal candidate for this model, with 99.9% of proton transfers occurring by tunneling from the RTE, 43.5 kJ mol^{-1} below the top of the barrier.[13]

The solution for this model at 298 K for which the gating frequency is ω_X = 165 cm^{-1} and KIE = 55 (Figure 3) corresponds to a weak temperature dependence of the KIE ($\Delta\Delta H^{\ddagger}$ = 3.7 kJ mol^{-1}), well within the experimental error (~5 kJ mol^{-1}) from our kinetic studies[13] (see Methods). Additionally, there is reasonable agreement between the calculated (determined from Supporting Information Figure S3) and experimental[13] values for $\ln(A'_H)$ (23.0 and 25.6 ± 1.4, respectively) and $\ln(A'_D)$ (20.5 and 19.8 ± 0.5, respectively). The r_0 value, 0.64 Å, is 0.05 Å greater than the tunneling distance (0.59 Å[13]), which is in accord with the calculated 0.05 Å rms deviation for this gating mode (eq 13). Despite being significantly shorter than the equilibrium well separation [d(O2−H1) = 2.67 Å],[13] this is reasonable, since r_0 is not the equilibrium well separation but the separation at a nuclear configuration compatible with tunneling. This strongly suggests that the tunneling kinetics of AADH are not driven purely by collective thermally equilibrated dynamical motions. On the basis of similar calculations for the tunneling reaction in soybean lipoxygenase (SLO), Klinman and co-workers have suggested that temperature-independent KIEs are not consistent with a strongly gated tunneling step and that a thermally active gating mode ($\hbar\omega_X \leq k_BT$, $\omega_X \leq$ 220 cm^{-1}) leads to temperature-dependent KIEs with an inverse ratio of Arrhenius prefactors ($A_H/A_D \ll 1$).[20] However, after fitting our model to the experimental data (Supporting Information Figure S3; employing the Eyring equation[54]) using the values in Table 1 and the rate expression in eq 9,[20] an A'_H/A'_D value[54] of 11.8 was obtained (fitting to the Arrhenius equation, an A_H/A_D value of 11.8 was obtained). This illustrates that experimentally observed KIEs that are essentially temperature-independent (i.e., not measurably temperature-dependent) are consistent with a sub-picosecond promoting vibration along the reaction coordinate which assists the tunneling process. On the other hand, modeling the experimental data by invoking tunneling through a static barrier (Table 1), both with and without the involvement of excited vibrational states, requires a r value (i.e., a tunneling distance) that is significantly shorter than the computationally derived value.[13]

A recent refinement of the Kuznetsov and Ulstrup model is the replacement of the harmonic oscillator by an anharmonic Morse potential, which, for a given KIE and $\Delta\Delta H^{\ddagger}$, decreases ω_X and increases r_0.[8] However, the harmonic model employed here can accommodate both significantly higher frequencies and lower r_0 values; thus, similar ω_X and r_0 values can presumably be obtained using an anharmonic model.

The numerical calculations performed in this work employed an m_X value of 100 Da, which is similar to that used by Klinman and co-workers[20,55] and is the approximate mass of one amino acid residue (it should be noted that m_X is in fact a reduced mass and not the absolute mass of the motile atoms involved in the gating motion). However, m_X can always be adjusted to accommodate any given ω_X value by altering the force constant, k_{HO}, of the harmonic oscillator; this also affects $\Delta\Delta H^{\ddagger}$ and r_0. Therefore, to determine if the m_X value used fits with the experimental data and the computationally derived frequency as well as the computationally derived tunneling distance, the

KIE was fixed at 55, ω_X was fixed at 165 cm^{-1}, and k_{HO} was systematically altered. From these calculations, a lower limit of 70 Da for m_X and an upper limit of 0.7 Å for r_0 were defined (Supporting Information Figures S4 and S5). The upper limit on m_X is 1000 Da; as the mass increases to this value, $\Delta\Delta H^{\ddagger}$ converges to 0 and r_0 converges to 0.51 Å, the tunneling distance through a static barrier (i.e., the case when no gating is involved).

In the extensively studied enzyme dihydrofolate reductase (DHFR), a network of coupled long-range motions, corresponding to regions of strong cross-correlation,[42] has been proposed to drive the tunneling event.[10,35,56] There is also evidence for the involvement of long-range dynamical effects in liver alcohol dehydrogenase (LADH).[45,57−60] There is no network of strong cross-correlation observed in AADH (Supporting Information Figure S2), suggesting that coupled long-range motions are likely to be less significant in AADH. The promoting vibraton that has been identified for AADH, which arises from the coupling of a vibration within the proton donor group to the vibration of the acceptor atom, appears at variance with these results. There are, however, significant differences between the tunneling reaction catalyzed by AADH and those catalyzed by DHFR and LADH, which might explain the different levels of involvement of enzyme dynamics. Perhaps the most obvious difference is that, while they all involve the breaking of a carbon−hydrogen bond, the former involves transfer of a proton whereas the latter two involve transfer of a hydride. A proton transfer may be facilitated by withdrawal of electron density from the donor−hydrogen bond, which polarizes and weakens the C−H bond. In AADH, this effect is assisted by the electron poor iminoquinone, facilitating a favorable electrostatic interaction—or even formation of a hydrogen bond—between the strongly polarized C1/H1 and the negatively charged O2, which helps couple the vibration of C1/H1 to O2. In DHFR and LADH, the vibrations of the donor or acceptor groups will not be so readily coupled, because a hydride transfer cannot be facilitated by such an effect—a partial negative charge will not reside on the transferring hydrogen. Therefore, a promoting vibration cannot arise from electrostatic interactions developing between the donor and acceptor groups and will instead require mechanical effects to drive the donor and acceptor groups together.

The 165 cm^{-1} promoting vibration identified in AADH arises from the flexibility of the linker region connecting the indole and quinone. In contrast, the substrates of DHFR and LADH have less flexible donor and acceptor functional groups; the hydride transfer in DHFR occurs between nicotinamide adenine nucleotide phosphate (NADPH) and dihydrofolate (DHF), and that in LADH, between benzyl alcoxide and NAD^+. This means that a motion that drives the donor and acceptor groups together is more likely to involve large portions of the donor and/or acceptor, driven by forces external to these regions. Furthermore, substrates and cofactors in DHFR and LADH are not covalently bound to the enzymes, as is the case in AADH, so that the donor and acceptor groups are replaced in subsequent catalytic cycles. In AADH, on the other hand, once the iminoquinone has been reduced, the gained electron is transferred to the electron acceptor protein azurin. Because of the evolutionary pressure to interact effectively with azurin, as well as the complexity of the mechanism of the reaction catalyzed by AADH,[13] it is less likely that AADH would also have evolved to utilize large-scale motions to drive the proton transfer step.

Conclusions

A promoting vibration, with a frequency of ∼165 cm^{-1}, has been identified for the proton tunneling step in the oxidative deamination of tryptamine catalyzed by AADH. This vibration does not require large-scale dynamics of the protein scaffold but is inherent to the proton donor, the iminoquinone intermediate. This promoting vibration corresponds to a rotation of the donor C1/H1 methylene group, which couples to the acceptor oxygen, O2, so that these atoms all move toward a configuration from which tunneling becomes more probable. This result indicates that—in addition to being mechanistically, thermodynamically, and kinetically favored—proton transfer to O2 is dynamically favored. Motions other than this promoting vibration (i.e., preorganization) are likely involved in moving the system toward a tunneling-ready configuration, from which the gating motion can take effect, for example, the repositioning of O2 which could bring O2 sufficiently close to H1 for an electrostatic coupling of their respective vibrations to occur. We wish to emphasize that, although the absolute rates and the temperature dependence of these rates depend on such motions, $\Delta\Delta H^{\ddagger}$ and the temperature dependence of the KIE depend on the gating term. This was identified as a specific sub-picosecond vibration involving the coupled vibrations of the donor, acceptor, and transferring proton along the reaction coordinate, consistent with the Kuznetsov and Ulstrup model for H-tunneling and an observed KIE that is not measurably temperature-dependent.

Acknowledgment. This work was funded by the UK Biotechnology and Biological Sciences Research Council (BBSRC) and the University of Leicester. N.S.S. is a BBSRC Professorial Research Fellow.

Supporting Information Available: Table, figures, and a more detailed description of the coupling and correlations (eq 1) further supporting the text. This material is available free of charge via the Internet at http://pubs.acs.org.

References and Notes

(1) Ball, P. *Nature* **2004**, *431*, 396.
(2) Hwang, J. K.; Chu, Z. T.; Yadav, A.; Warshel, A. *J. Phys. Chem.* **1991**, *95*, 8445.
(3) Hwang, J. K.; Warshel, A. *J. Am. Chem. Soc.* **1996**, *118*, 11745.
(4) Olsson, M. H.; Siegbahn, P. E.; Warshel, A. *J. Am. Chem. Soc.* **2004**, *126*, 2820.
(5) Doll, K. M.; Bender, B. R.; Finke, R. G. *J. Am. Chem. Soc.* **2003**, *125*, 10877.
(6) Doll, K. M.; Finke, R. G. *Inorg. Chem.* **2003**, *42*, 4849.
(7) Siebrand, W.; Smedarchina, Z. *J. Phys. Chem. B* **2004**, *108*, 4185.
(8) Kohen, A.; Klinman, J. P. *Acc. Chem. Res.* **1998**, *31*, 397.
(9) Villa, J.; Warshel, A. *J. Phys. Chem. B* **2001**, *105*, 7887.
(10) Benkovic, S. J.; Hammes-Schiffer, S. *Science* **2003**, *301*, 1196.
(11) Hammes-Schiffer, S.; Benkovic, S. J. *Annu. Rev. Biochem.* **2006**, *75*, 519.
(12) Benkovic, S. J.; Hammes-Schiffer, S. *Science* **2006**, *312*, 208.
(13) Masgrau, L.; Roujeinikova, A.; Johannissen, L. O.; Hothi, P.; Basran, J.; Ranaghan, K. E.; Mulholland, A. J.; Sutcliffe, M. J.; Scrutton, N. S.; Leys, D. *Science* **2006**, *312*, 237.
(14) Knapp, M. J.; Klinman, J. P. *Eur. J. Biochem.* **2002**, *269*, 3113.
(15) Basran, J.; Sutcliffe, M. J.; Scrutton, N. S. *Biochemistry* **1999**, *38*, 3218.
(16) Basran, J.; Patel, S.; Sutcliffe, M. J.; Scrutton, N. S. *J. Biol. Chem.* **2001**, *276*, 6234.
(17) Harris, R. J.; Meskys, R.; Sutcliffe, M. J.; Scrutton, N. S. *Biochemistry* **2000**, *39*, 1189.
(18) Basran, J.; Harris, R. J.; Sutcliffe, M. J.; Scrutton, N. S. *J. Biol. Chem.* **2003**, *278*, 43973.
(19) Kohen, A.; Cannio, R.; Bartolucci, S.; Klinman, J. P. *Nature* **1999**, *399*, 496.
(20) Knapp, M. J.; Rickert, K.; Klinman, J. P. *J. Am. Chem. Soc.* **2002**, *124*, 3865.

(21) Francisco, W. A.; Knapp, M. J.; Blackburn, N. J.; Klinman, J. P. *J. Am. Chem. Soc.* **2002**, *124*, 8194.
(22) Agrawal, N.; Hong, B.; Mihai, C.; Kohen, A. *Biochemistry* **2004**, *43*, 1998.
(23) Sikorski, R. S.; Wang, L.; Markham, K. A.; Rajagopalan, P. T. R.; Benkovic, S. J.; Kohen, A. *J. Am. Chem. Soc.* **2004**, *126*, 4778.
(24) Maglia, G.; Allemann, R. K. *J. Am. Chem. Soc.* **2003**, *125*, 13372.
(25) Swanwick, R. S.; Maglia, G.; Tey, L. H.; Allemann, R. K. *Biochem. J.* **2006**, *394*, 259.
(26) Bell, R. P. The application of tunnel corrections in chemical kinetics. *The Tunnel Effect in Chemistry*; Chapman and Hall: London, 1980; p 51.
(27) Kuznetsov, A. M.; Ulstrup, J. *Can. J. Chem.* **1999**, *77*, 1085.
(28) Truhlar, D. G.; Gao, J. L.; Garcia-Viloca, M.; Alhambra, C.; Corchado, J.; Sanchez, M. L.; Poulsen, T. D. *Int. J. Quantum Chem.* **2004**, *100*, 1136.
(29) Alhambra, C.; Corchado, J.; Sanchez, M.; Gao, J.; Truhlar, D. *J. Am. Chem. Soc.* **2000**, *122*, 8197.
(30) Faulder, P. F.; Tresadern, G.; Chohan, K. K.; Scrutton, N. S.; Sutcliffe, M. J.; Hillier, I. H.; Burton, N. A. *J. Am. Chem. Soc.* **2001**, *123*, 8604.
(31) Alhambra, C.; Sanchez, M. L.; Corchado, J.; Gao, J. L.; Truhlar, D. G. *Chem. Phys. Lett.* **2001**, *347*, 512.
(32) Alhambra, C.; Sanchez, M. L.; Corchado, J.; Gao, J.; Truhlar, D. G. *Chem. Phys. Lett.* **2002**, *355*, 388.
(33) Tresadern, G.; Wang, H.; Faulder, P. F.; Burton, N. A.; Hillier, I. H. *Mol. Phys.* **2003**, *101*, 2775−2784.
(34) Nunez, S.; Tresadern, G.; Hillier, I. H.; Burton, N. A. *Philos. Trans. R. Soc. London, Ser. B* **2006**, *361*, 1387.
(35) Agarwal, P. K.; Billeter, S. R.; Rajagopalan, P. T.; Benkovic, S. J.; Hammes-Schiffer, S. *Proc. Natl. Acad. Sci. U.S.A.* **2002**, *99*, 2794.
(36) Pu, J. Z.; Ma, S. H.; Gao, J. L.; Truhlar, D. G. *J. Phys. Chem. B* **2005**, *109*, 8551.
(37) Pang, J.; Pu, J.; Gao, J.; Truhlar, D. G.; Allemann, R. K. *J. Am. Chem. Soc.* **2006**, *128*, 8015.
(38) Garcia-Viloca, M.; Gao, J.; Karplus, M.; Truhlar, D. G. *Science* **2004**, *303*, 186.
(39) Hammes-Schiffer, S. *Curr. Opin. Struct. Biol.* **2004**, *14*, 192.
(40) Masgrau, L.; Basran, J.; Hothi, P.; Sutcliffe, M. J.; Scrutton, N. S. *Arch. Biochem. Biophys.* **2004**, *428*, 41.
(41) Tresadern, G.; Nunez, S.; Faulder, P. F.; Wang, H.; Hillier, I. H.; Burton, N. A. *Faraday Discuss.* **2003**, *122*, 223.
(42) Radkiewicz, J. L.; Brooks, C. L. *J. Am. Chem. Soc.* **2000**, *122*, 225.
(43) Caratzoulas, S.; Mincer, J. S.; Schwartz, S. D. *J. Am. Chem. Soc.* **2002**, *124*, 3270.
(44) Sessions, R. B.; Dauber-Osguthorpe, P.; Osguthorpe, D. J. *J. Mol. Biol.* **1989**, *210*, 617.
(45) Mincer, J. S.; Schwartz, S. D. *J. Phys. Chem. B* **2003**, *107*, 366.
(46) Caratzoulas, S.; Schwartz, S. D. *J. Chem. Phys.* **2001**, *114*, 2910.
(47) Benderskii, V. A.; Makarov, D. E.; Wight, C. A. *Chemical Dynamics at Low Temperatures*; Advances in Chemical Physics, Vol. 88; Wiley: New York, 1994.
(48) Antoniou, D.; Schwartz, S. D. *J. Chem. Phys.* **1998**, *108*, 3620.
(49) Antoniou, D.; Schwartz, S. D. *J. Phys. Chem. B* **2001**, *105*, 5553.
(50) Hatcher, E.; Soudackov, A. V.; Hammes-Schiffer, S. *J. Am. Chem. Soc.* **2004**, *126*, 5763.
(51) Agarwal, P. K.; Billeter, S. R.; Hammes-Schiffer, S. *J. Phys. Chem. B* **2002**, *106*, 3283.
(52) Wong, K. F.; Watney, J. B.; Hammes-Schiffer, S. *J. Phys. Chem. B* **2004**, *108*, 12231.
(53) Siegbahn, P. E. *Q. Rev. Biophys.* **2003**, *36*, 91.
(54) Arrhenius plots are curved and as such asymptotically approach infinity at high temperatures. It is therefore strictly correct to use the Eyring equation to analyze the temperature dependence of rate constants: $\ln(k/T) = \ln A' - \Delta H^{\ddagger}/RT$, $\ln A' = \ln(k_B/h) + \Delta S^{\ddagger}/R$. Here, A' is analogous to the Arrhenius prefactor, A.
(55) Meyer, M. P.; Klinman, J. P. *Chem. Phys.* **2005**, *319*, 283.
(56) Sutcliffe, M. J.; Scrutton, N. S. *Phys. Chem. Chem. Phys.* **2006**, *8*, 4510.
(57) Bahnson, B. J.; Park, D. H.; Kim, K.; Plapp, B. V.; Klinman, J. P. *Biochemistry* **1993**, *32*, 5503.
(58) Bahnson, B. J.; Colby, T. D.; Chin, J. K.; Goldstein, B. M.; Klinman, J. P. *Proc. Natl. Acad. Sci. U.S.A.* **1997**, *94*, 12797.
(59) Chin, J. K.; Klinman, J. P. *Biochemistry* **2000**, *39*, 1278.
(60) Mincer, J. S.; Schwartz, S. D. *J. Proteome Res.* **2003**, *2*, 437.